RESEARCH ACTIVITIES II
Department of Molecular Structure

II-A Development of Near-Field Dynamic Spectroscopy and Application to Nanometric Systems

There is much demand for the study of local optical properties of molecular assemblies and materials, to understand mesoscopic phenomena and/or to construct optoelectronic devices in nanometric scale. Scanning near-field optical microscopy (SNOM), which enables spatial resolution beyond the diffraction limit of light, shows remarkable progress in technology in these days. Combination of this advanced optical technology with ultrafast spectroscopic methods may offer a direct probe of molecular dynamical processes in mesoscopic systems. It may bring essential and basic knowledge for analyzing origins of characteristic features and functionalities of mesoscopic systems. We are constructing apparatus for near-field dynamic spectroscopy with femtosecond temporal resolution and nanometer spatial resolution. Using the apparatus developed, we have observed characteristic spatiotemporal behavior of various organic molecular systems and metal nanoparticles, for the purpose of understanding spatial coherence and dissipation of excitations and their dynamics. Outlines of the construction and experimental results obtained are summarized here.

II-A-1 Scanning Near-Field Optical Microscopy with Supercontinuum Light Pulses Generated in Microstructure Fiber

NAGAHARA, Tetsuhiko; IMURA, Kohei; OKAMOTO, Hiromi

[*Rev. Sci. Instrum.* **75**, 4528–4533 (2004)]

We have utilized supercontinuum (SC) pulses as a light source for SNOM experiments with high spatial-resolution (~ 100 nm) determined by the aperture size of the near-field probe. The SC ranging from 560 nm to > 1 μm is generated by focusing mode-locked Ti: sapphire laser pulses into a microstructure fiber. The continuum can be used as a wavelength-tunable light source for fluorescence excitation as well as for probing absorption of excited states.

To examine performance and versatility of the apparatus, fluorescence image of pseudoisocyanine J-aggregate was measured. The sample was illuminated through the apertured tip by spectrally-sliced SC at 560 nm. Fluorescence from the sample (at 590 nm) was detected by an avalanche photodiode. Fluorescence (Figure 1A) and topographic (not shown) images correlate very well. The images show that the J-aggregates have fibrous structures, in agreement with earlier works. The fluorescence image is in some parts noisy and smeared. The noisy signal is coming from fluctuation of the SC, and quality of the fluorescence image would be much improved by stabilizing the incident Ti:sapphire laser.

Next we describe two-color pump-probe measurements using SC. Time resolution in the near-field with near-IR probe pulse was in 1–2 ps range, while that with 570 nm pulse was 5 ps without pre-compensation of group delay dispersion. As an example, we have measured a thin film of porphyrin J-aggregates. Signals from spectrally sliced SC at 810 nm after excitations at 780 nm are shown in Figure 1C, together with the topography (Figure 1B) of the sample. The lifetimes at positions specified in the topograph (112 ± 6 ps and 79 ± 6 ps) show clear site dependence. The site-specificities in excited-state dynamics have been revealed in the present *two-color* experiment much more clearly compared to our previous *one-color* result,1) since the baselines are directly determined from intensities at negative delay times.

Reference

1) T. Nagahara, K. Imura and H. Okamoto, *Chem. Phys. Lett.* **381**, 368–375 (2003).

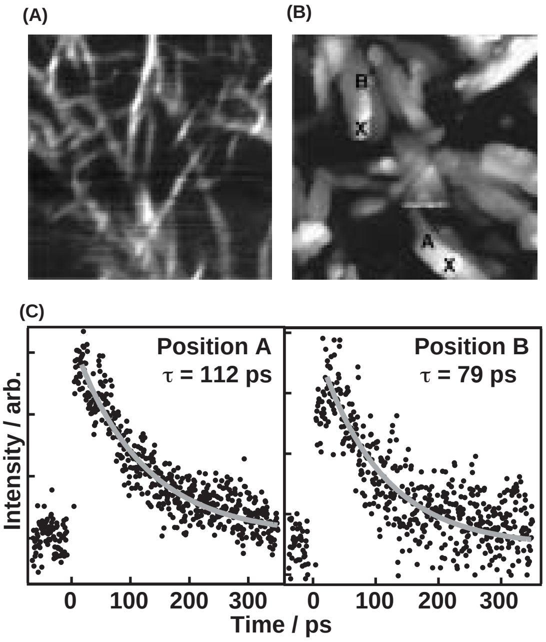

Figure 1. (A) Fluorescence image of PIC J-aggregate detected at 590 nm. Scan range: 10 μm × 10 μm. (B) Topography of tetrakis(4-methoxyphenyl)porphyrin J-aggregate. Scan range: 5 μm × 5 μm. (C) Signals obtained by 780-nm pump / 810-nm probe experiments and their fit to exponential function.

II-A-2 Near-Field Spectroscopy of Water-Soluble and Water-Insoluble Porphyrin J-Aggregates

NAGAHARA, Tetsuhiko; IMURA, Kohei; OKAMOTO, Hiromi

[*Scanning* **26** (Suppl. I), 10–15 (2004)]

Recently, we examined the mesoscopic structures and spatial inhomogeneities of J-aggregate of water-insoluble tetrakis(4-methoxyphenyl)porphyrin (TMe OPP) in thin film by SNOM. The results obtained were as follows: (a) thin film consists of bundles of long and planer microcrystalline structures; (b) site-specific transmittance spectra might reflect spatial inhomogeneity of the sample, which may be a major origin of the broad J-bands in the far-field spectrum. However, influence of substituent groups on the spatial inhomogeneities and morphologies was not investigated. In the present study, we have studied mesoscopic structures and optical properties of J-aggregates of tetraphenylporphyrins with different substituent groups [unsubstituted (TPP) and 4-sulfonated (TSPP)].

From topographic images, TSPP sample is composed of needle-like planar microcrystals (~1 μm-L, ~100 nm-W and 5–10 nm-H), while that of TPP (Figure 1B) shows stacks of planer (300 ~ 600 nm × 300 ~ 600 nm, ~ 20 nm-H) microcrystalline structures. From polarized transmittance images of TSPP (Figure 1A), it was found that a large transition moment is parallel to the long crystalline axis. Individual microcrystallines in TPP sample have been found to be planer rhomboid structures by SEM observations. Such morphological differences are probably due to microscopic differences in aggregate structures.

In the far-field absorption and fluorescence spectra, the bandwidths of the water-insoluble samples (TPP and TMeOPP) were much broader than that of water-soluble sample (TSPP), suggesting serious contributions of inhomogeneous broadening. The near-field transmittance spectra of the water-insoluble samples show strong site-dependence (Figure 1C), while those of the water-soluble ones do not. The origin of the broad absorption band observed in water-insoluble samples can be ascribed to spatial inhomogeneities.

Reference

1) T. Nagahara, K. Imura and H. Okamoto, *Chem. Phys. Lett.* **381**, 368–375 (2003).

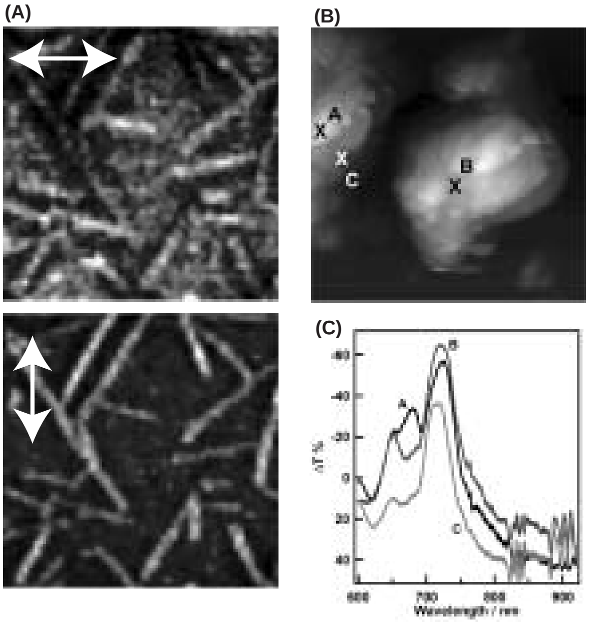

Figure 1. (A) Polarized transmittance image of TSPP J-aggregate. Arrows indicate polarization directions. Scan range: 2 μm × 2 μm. (B) Surface topography of TPP J-aggregate. Scan range: 5 μm × 5 μm. (C) Transmittance difference spectra at positions indicated in (B).

II-A-3 Near-Field Optical Observation of Gold Nanoparticles

IMURA, Kohei; NAGAHARA, Tetsuhiko; OKAMOTO, Hiromi

[*Chem. Phys. Lett.* **400**, 500–505 (2004)]

Optical properties of noble metal particles have been widely investigated because of fundamental importance in science and in industry. Not only the local field enhancement but also the SP mode behaviors in near-field arouse fundamental interests and various applications. Wavelength-dependent characteristics of SP modes on metal nanoparticles are essential for utilizing them as novel optical and electronic materials, and also for constructing molecular systems for nanophotonic applications as well.

We investigated interaction between evanescent wave and a single gold nanoparticle in near-field by utilizing an aperture-probe SNOM. A characteristic spectral feature, consisting of transmission enhancement and absorptive parts, was found. Observed spectra were successfully simulated by a model calculation based on extended Mie scattering theory of the near- and far-field scatterings as well as by a Green dyadic treatment of electromagnetic field.

II-A-4 Two-Photon Induced Photoluminescence Imaging of Single Gold Particles

IMURA, Kohei; NAGAHARA, Tetsuhiko; OKAMOTO, Hiromi

[*J. Am. Chem. Soc.* **126**, 12730–12731 (2004)]

Strong field confinement near and/or adjacent particles is important in surface enhanced Raman scattering (SERS). However, knowledge about spatial distribution of electric field near the particle and how plasmon modes play roles in the particle are still not fully understood. We have found that two-photon induced photoluminescence (TPI-PL) of single nanoparticles can be excited in the near-field, and this has been used to reveal spatial distribution of electric field near the particle as well as spatial characteristics of plasmon modes.

Gold nanoparticles were synthesized chemically in solutions by seed-mediated method. Morphology of the sample was verified by topography measurements by the apertured SNOM and/or by a scanning electron microscope. Samples were spin-coated on a cover-slip. A Ti:sapphire laser (λ = 780 nm, < 100 fs) was used to excite TPI-PL. Laser power dependence measurement of the PL intensity confirmed that PL was due to a two-photon induced process.

Figure 1 (a,b) shows the TPI-PL image of single gold nanorods. Figure 1(a) shows electric field enhancement near the ends of the rod, while Figure 1(b) shows a characteristic spatial oscillation. This oscillatory behavior is well reproduced by an electromagnetic calculation and is ascribed to electromagnetic local density of states which reflect the eigenfunction of certain surface plasmon mode. The origin of the difference between Figures 1(a) and (b) is possibly related to microscopic edge structures of the rod and/or the resonance condition of the plasmon mode at the excitation wavelength.

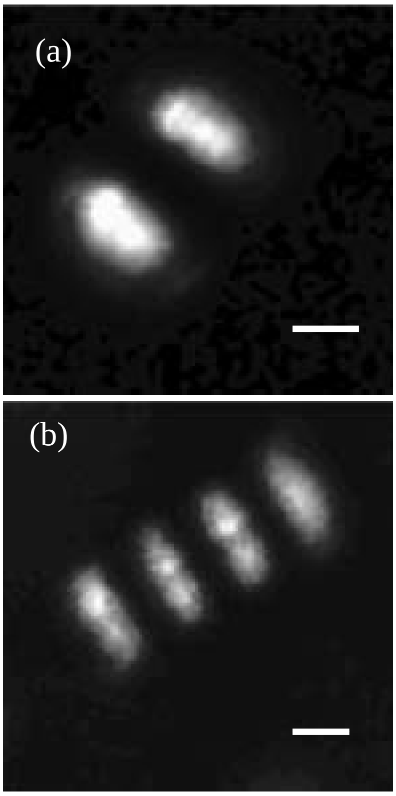

Figure 1. (a,b) Two-photon induced PL images for two typical single gold nanorods. Scale bars are 100 nm.

II-A-5 Ultrafast Near-Field Imaging of Single Gold Nanorods

IMURA, Kohei; NAGAHARA, Tetsuhiko; OKAMOTO, Hiromi

[*J. Phys. Chem. B* **108**, 16344–16347 (2004)]

We deal with ultrafast dynamics of collective oscillation of electrons, known as surface plasmon (SP), for gold nanorods. The SP modes of nanoparticles give rise to strong interaction with photons. It is of fundamental importance to know how the electron-electron and electron-phonon scattering processes after photoexcitation depend upon size and shape of nanoparticles and how they proceed inside the particle. Dynamical spectroscopy of a single particle with high temporal and spatial resolution must be informative for this purpose. We have performed experiments of ultrafast near-field pump-probe imaging, and investigated the dynamic behavior of the excited particle in a space- and time-resolved manner.

Figure 1 shows transient transmission images of a gold nanorod taken at various pump-probe delay times. As it is clearly seen in the figure, temporal response of central part of the particle is different from those of the both ends. A fast rise and a slow decay are seen for the ends parts, while only a fast rise component is observed for the central part. The time constant for the faster component was found 0.6 ± 0.1 ps and the slower one 2.8–1.5 ps depending on the position inside the particle. The faster and slower components are assigned to electron-electron and electron-phonon scattering, respectively. It is found that the electron-phonon relaxation becomes faster towards the end edge of the nanorod.

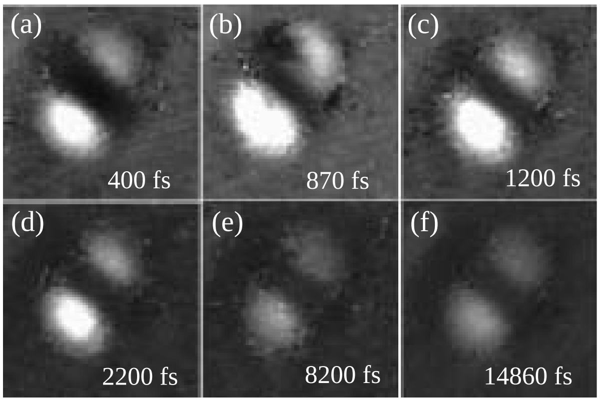

Figure 1. (a–f) Transient transmission images of a gold nanorod taken at various pump-probe delay times (indicated in each image). Scan range: 600 nm × 600 nm.